

**Rhenium and technetium-complexed silicon rhodamines as near-infrared imaging probes for bimodal SPECT- and optical imaging**

Kanagasundaram, T.; Kramer, C. S.; Boros, E.; Kopka, K.;

Originally published:

May 2020

**Dalton Transactions 64(2020), 7294-7298**

DOI: <https://doi.org/10.1039/D0DT01084G>

Perma-Link to Publication Repository of HZDR:

<https://www.hzdr.de/publications/Publ-30839>

Release of the secondary publication  
on the basis of the German Copyright Law § 38 Section 4.

# Dalton Transactions

An international journal of inorganic chemistry

Accepted Manuscript

This article can be cited before page numbers have been issued, to do this please use: T. Kanagasundaram, C. S. Kramer, E. Boros and K. Kopka, *Dalton Trans.*, 2020, DOI: 10.1039/D0DT01084G.



This is an Accepted Manuscript, which has been through the Royal Society of Chemistry peer review process and has been accepted for publication.

Accepted Manuscripts are published online shortly after acceptance, before technical editing, formatting and proof reading. Using this free service, authors can make their results available to the community, in citable form, before we publish the edited article. We will replace this Accepted Manuscript with the edited and formatted Advance Article as soon as it is available.

You can find more information about Accepted Manuscripts in the [Information for Authors](#).

Please note that technical editing may introduce minor changes to the text and/or graphics, which may alter content. The journal's standard [Terms & Conditions](#) and the [Ethical guidelines](#) still apply. In no event shall the Royal Society of Chemistry be held responsible for any errors or omissions in this Accepted Manuscript or any consequences arising from the use of any information it contains.

## COMMUNICATION

## Rhenium and technetium-complexed silicon rhodamines as near-infrared imaging probes for bimodal SPECT- and optical imaging

Thines Kanagasundaram<sup>ab</sup>, Carsten S. Kramer<sup>a</sup>, Eszter Boros<sup>\*†c</sup> and Klaus Kopka<sup>\*†d</sup>Received 00th January 20xx,  
Accepted 00th January 20xx

DOI: 10.1039/x0xx00000x

**Fluorescent Si-rhodamines were modified to enable complexation with the Re(I)- and <sup>99m</sup>Tc(I)-tricarbonyl core. The corresponding complexes exhibit suitable properties as bimodal imaging probes for SPECT- and optical imaging *in vitro*. Importantly, the novel in aqueous solution stable, functionalized Si-rhodamines retain favourable optical properties after complexation ( $QY=0.09$ ,  $\lambda_{abs}=654$  nm,  $\lambda_{em}=669$  nm in PBS) and show promising near-infrared optical properties for potential *in vivo* applications enabling bimodal scintigraphic imaging and optical imaging, e.g. used in radio- and fluorescence-guided tumor resection.**

Organic fluorophores are in high demand as imaging probes in biomedical research.<sup>1, 2</sup> Optical dyes are generally used for cellular staining, biomolecule characterisation or the visualization of cellular and molecular processes *in vivo*.<sup>3-5</sup> The most extensively studied organic fluorescent dyes for biological applications are fluorescein, squaraine-, BODIPY- and cyanine-dyes (figure 1).<sup>1, 6</sup> At this time, the FDA approved fluorophores indocyanine green (ICG) and 5-aminolevulinic acid (5-ALA) are the most established compounds for intraoperative surgical interventions.<sup>7</sup> These organic dyes possess high molar extinction coefficients, large Stokes shifts and high quantum yields.<sup>1</sup> However, in exception of some fluorophores with reduced molecular weight, most of the dyes e.g. members of the FITC family, typically show limited optical properties not compatible with *in vivo* applications due to their

absorbance and emission in the visible part of the spectrum since their absorbance and emission maxima interfere with the natural absorbance of tissue and blood.<sup>6, 8-11</sup> In contrast, NIR dyes do not overlap with the absorbance of water and haemoglobin, and provide low phototoxicity in cells and tissue.<sup>8</sup> These advantages qualify near-infrared (NIR) dyes particularly powerful for optical imaging. The indocyanine (Cy) dye family provides a suitable alternative to bright, short wave optical probes, as emission properties can be adjusted to NIR compatibility by chain extension. However, indocyanines exhibit decreased solubility in aqueous solution and are sensitive to photobleaching, which can pose limitations to their application.<sup>6</sup> Clearly, there is a need for optical probes with small molecular footprint, necessary hydrophilicity for biological applications and strongly red-shifted absorbance and emission. In 2011 Nagano et al. developed the near-infrared silicon rhodamines (SiR) with a maximal absorption wavelength of  $\lambda_{abs}=646$  nm and an emission wavelength of  $\lambda_{em}=667$  nm (figure 1).<sup>5, 12, 13</sup> Due to their optical properties in the near-infrared wavelength region the SiR dyes exhibit biocompatible characteristics: enhanced photostability and water solubility, reduced autofluorescence, decreased light scattering- and photobleaching properties.<sup>5, 12, 13</sup>

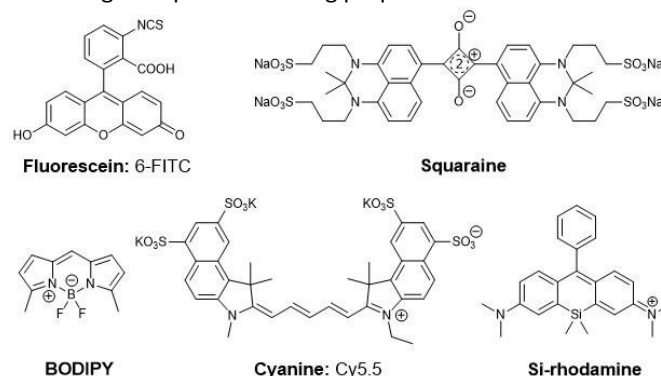


**Figure 1:** Overview of prominent organic fluorescent dyes and chemical structures of fluorescein, squaraine-, BODIPY-, cyanine and silicon-rhodamine dyes.

<sup>a</sup> Division of Radiopharmaceutical Chemistry, German Cancer Research Center (DKFZ), Im Neuenheimer Feld 223, 69120 Heidelberg, Germany.

<sup>b</sup> Institute of Inorganic Chemistry, Heidelberg University, Im Neuenheimer Feld 270, 69120 Heidelberg, Germany.

<sup>c</sup> Department of Chemistry, Stony Brook University, 100 Nicolls Road, Stony Brook, New York 11790, United States.

E-mail: eszter.boros@stonybrook.edu

<sup>d</sup> Helmholtz-Zentrum Dresden-Rossendorf (HZDR) e.V., Institute of Radiopharmaceutical Cancer Research, Bautzner Landstrasse 400, 01328 Dresden, Germany.

E-mail: k.kopka@hzdr.de

† Both authors share senior last authorship.

Electronic Supplementary Information (ESI) available: [details of any supplementary information available should be included here]. See DOI: 10.1039/x0xx00000x

Molecular imaging methods with optical imaging probes are used extensively for the visualization of cellular processes.<sup>3-5</sup> Although this method is considered to also provide high spatial resolution in the  $\mu\text{m}$ -scope and high sensitivity *in vivo*, the lack of deep tissue penetration can be compensated by use of complementary imaging techniques.<sup>14</sup> Nuclear imaging methods such as positron emission tomography (PET) and single photon emission computed tomography (SPECT)-imaging are suitable for this purpose due to their tissue penetration characteristics and high sensitivity suitable for whole body imaging.<sup>15</sup> Conclusively the combination of optical and nuclear imaging methods provides synergistic effects, resulting in high spatial resolution and high tissue penetration from the whole body to the subcellular level.<sup>15-17</sup> Related to this topic several small molecule based organic optical- and nuclear imaging probes have been evaluated and reported.<sup>18</sup> However fluorescent dyes including radiolabelled and functionalized BODIPYs, cyanine or fluorescein-conjugated imaging probes often show a low accumulation in tumors likely because of their enhanced lipophilicity and high enrichment in kidney or liver.<sup>17, 19-23</sup> For this reason there is a need of small molecule based water-soluble near-infrared absorbing and emitting probes for bimodal imaging and subsequent fluorescence-guided surgery.

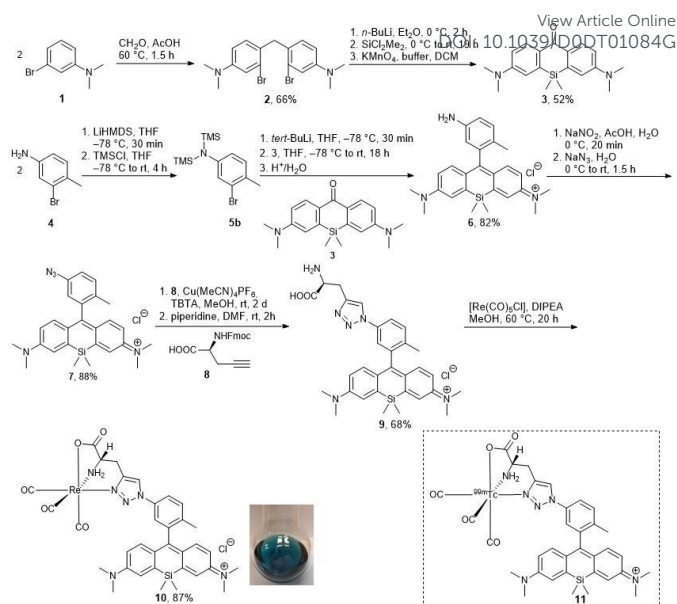
Here, we used the click-to-chelate concept from Mindt et al. to combine the single-photon emitter technetium-99m (physical half-life of 6.02 hours and gamma energy of 141 keV) and the near-infrared fluorophore silicon-rhodamine in one small molecule for its further development for bimodal scintigraphic and optical imaging, e.g. used in radio- and fluorescence-guided intraoperative tumor resection.<sup>24, 25</sup>

In order to incorporate <sup>99m</sup>Tc(I) onto the SiR dye, we used a tridentate donor for the coordination of the <sup>99m</sup>Tc-tricarbonyl core. The synthesis of the non-radioactive rhenium surrogate complex **10** and the technetium-99m complex **11** was achieved from 3-bromo-*N,N*-dimethylaniline (**1**) within seven steps (Scheme 1).

An azido-functionalized Si-rhodamine **7** was converted by the copper(I)-catalyzed alkyne-azide cycloaddition (CuAAC) into the corresponding 1,4-substituted 1,2,3-triazole and subsequently complexed with rhenium(I) as a non-radioactive surrogate for chemical characterization.

To obtain dye **7**, we carried out the synthesis following the modification of published procedures: the commercially available 3-bromo-*N,N*-dimethylaniline (**1**) was converted using the Blanc reaction to compound **2**.<sup>26</sup> Using a modified procedure from Bertozzi et al., silicon-xanthone **3** was synthesized with a yield of 52%.<sup>27</sup> Xanthone **3** was converted by nucleophilic addition with trimethylsilyl-(TMS) protected anilines **5** to the amine-functionalized SiR **6**.<sup>28</sup>

Subsequently, SiR **6** was converted to the corresponding azide **7** with sodium azide. Formation of the corresponding 1,2,3-triazole-functionalized Si-rhodamine and subsequent complexation with Re(I) and Tc(I) were inspired by the click-to-chelate concept of Mindt et al.<sup>24, 29</sup> Various attempts at the copper(I)-catalyzed alkyne-azide click-reaction (CuAAC) conditions were carried out using Fmoc-*L*-propargylglycine **8** to



**Scheme 1:** Reaction pathway for the synthesis of the rhenium Si-rhodamine **10** and the structure of the technetium-99m radiolabelled Si-rhodamine **11**.

obtain the Fmoc-protected 1,4-disubstituted 1,2,3-triazole.

Reactions using conventional CuAAC conditions with copper(II) sulfate and sodium ascorbate were not successful; instead, we used the copper(I) source  $\text{Cu}(\text{MeCN})_4\text{PF}_6$  with tris((1-benzyl-4-triazolyl)methyl)amine (TBTA) in methanol.<sup>28</sup> This method gave the Fmoc-protected product in 87% yield. Finally, the Fmoc-group was removed using base-catalyzed deprotection in DMF to obtain **9** with a yield of 68%. The usage of unprotected *L*-propargylglycine as the alkyne source for the click reaction gave triazole **9** in an 18% yield only, possibly due to its diminished solubility in methanol. As Rhenium(I) and technetium(I)-complexes have often similar chemical properties, the rhenium complex **10** is considered as a suitable non-radioactive surrogate for the chemical characterization of the corresponding radioactive technetium-complex **11**.<sup>30</sup> Rhenium complex **10** was synthesized by complexation with pentacarbonylchlororhenium(I) with a yield of 87% after HPLC purification. The analytical HPLC showed a double peak signal which probably indicates two different rotameric structures of **10** (ESI-figure 47) due to the restricted rotation of the aryl-aryl axis from the Si-rhodamine backbone. The presence of rotamers is further evidenced by the HR-ESI-MS data from the double peak signal in HPLC, where one single mass of  $[\text{M}]^+$  with the correct isotopic pattern expected for <sup>185/187</sup>Re is observed. However only one set of chemical shift data was observed *via* NMR for this double signal at room temperature (ESI-figure 13/14).

A comparison of the proton <sup>1</sup>H-NMR data of the ligand **9** and the corresponding rhenium complex **10** indicates a downshift of signals following complexation, correlating well with previous published results (ESI-table 3).<sup>24, 29</sup>

This is further evidenced by the IR-data of complex **10**, which shows the well-defined and characteristic stretching frequency of CO bound to the rhenium core at  $\nu = 2022$  and  $1889\text{ cm}^{-1}$  (ESI-figure 44). The optical properties of all Si-rhodamine derivatives were determined in various solvents and are

shown in Table 1. With exception of **6** all other compounds show characteristic absorption- and emission properties in the NIR-region between 650 nm and 675 nm. The molar absorptivity of the SiRs in methanol is somewhat higher than in aqueous solution, and slightly decreases as the degree of substitution of the Si-rhodamines increases. The lowest molar absorption coefficients were obtained for the rhenium complex **10**, presumably by competing absorbance and emission from a metal-to-ligand charge-transfer (MLCT) band of the rhenium(II) complex; however, no further efforts were made to elucidate the source of observed change in molar absorptivity; comparable reduction of molar absorption coefficients following rhenium complexation with different fluorophores has been reported by others elsewhere.<sup>31-33</sup>

**Table 1** Optical properties of the synthesized Si-rhodamines and the Re-complex **10**. Excitation was performed at  $\lambda_{exc}$  = 650 nm.

	Solvent	$\lambda_{abs, max}$	$\lambda_{em}$	$\epsilon_{max}$	$\Phi_F$
<b>6</b>	MeOH	653 nm	-	91900 M <sup>-1</sup> cm <sup>-1</sup>	-
	PBS (pH = 7.4)	651 nm	-	77300 M <sup>-1</sup> cm <sup>-1</sup>	-
<b>7</b>	MeOH	651 nm	670 nm	156500 M <sup>-1</sup> cm <sup>-1</sup>	0.18
	H <sub>2</sub> O/EtOH (5%)	651 nm	670 nm	123700 M <sup>-1</sup> cm <sup>-1</sup>	0.10
	PBS (pH = 7.4)	651 nm	671 nm	99000 M <sup>-1</sup> cm <sup>-1</sup>	0.12
<b>9</b>	MeOH	655 nm	672 nm	79900 M <sup>-1</sup> cm <sup>-1</sup>	0.13
	H <sub>2</sub> O/EtOH (5%)	653 nm	671 nm	73890 M <sup>-1</sup> cm <sup>-1</sup>	0.10
	PBS (pH = 7.4)	655 nm	672 nm	79900 M <sup>-1</sup> cm <sup>-1</sup>	0.13
<b>10</b>	MeOH	654 nm	672 nm	63900 M <sup>-1</sup> cm <sup>-1</sup>	0.14
	H <sub>2</sub> O/EtOH (5%)	654 nm	674 nm	22100 M <sup>-1</sup> cm <sup>-1</sup>	0.10
	PBS (pH = 7.4)	654 nm	669 nm	39100 M <sup>-1</sup> cm <sup>-1</sup>	0.09

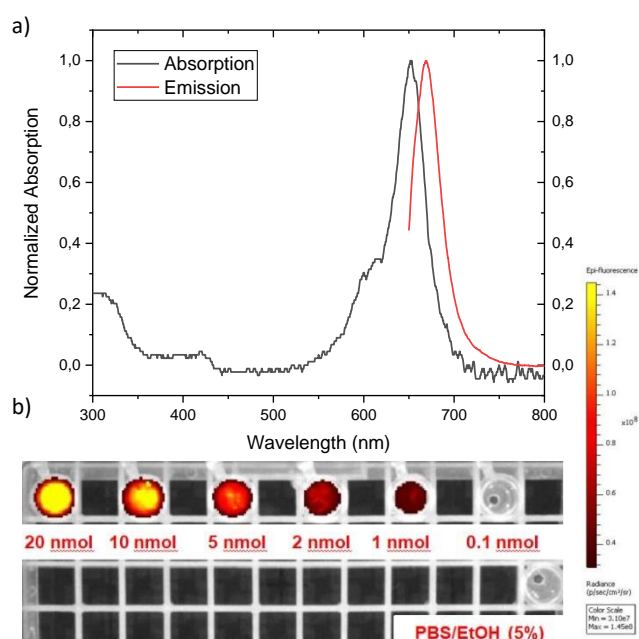


**Figure 2:** a) Normalized UV/VIS/NIR-absorption and emission spectrum of the rhenium complexed Si-rhodamine in water/ethanol (5%) with an excitation wavelength of 650 nm. b) IVIS-imaging of **10** in PBS/EtOH (5%) with different concentrations to receive the optimal amount of fluorophore for future *in vitro/in vivo* experiments. The samples were excited with a wavelength of 640 nm and the emission was recorded at a wavelength of 710 nm.

The Stokes shifts for all the dyes in methanol, PBS and H<sub>2</sub>O/EtOH (5%) remain comparable and small (15–20 nm), arising from a small and negligible change in dipole moment between the ground state and the excited state of the SiR

fluorophores. With exception of the non-fluorescent amine **6**, the quantum yields remain between 13–18% in MeOH and 9–13% in aqueous solution, respectively.

Figure 2a shows the absorption and emission spectra of the rhenium complex **10** in water/ethanol (5%).

The spectra show a maximum in absorbance at 654 nm and emission at 674 nm (excitation wavelength: 650 nm). Surprisingly, there is no significant change in quantum yield in H<sub>2</sub>O/EtOH (5%) between the ligand **9** and the rhenium complex **10** (both at  $\Phi_F$ =10%) while the molar absorption coefficient decreases dramatically from 73,890 to 22,100 M<sup>-1</sup>cm<sup>-1</sup>. The NIR-dyes **9** and **10** compare well to the FDA approved fluorescent dyes 5-aminolevulinic acid (5-ALA), protoporphyrin IX (PPIX;  $\Phi_F$ =8%) or the NIR-fluorophore indocyanine green (ICG;  $\Phi_F$ =9%) with respect to optical properties and solubility.<sup>7</sup>

Photobleaching experiments of the synthesized dyes **6**, **7**, **9** and **10** by irradiation with a wavelength of 650 nm from a xenon lamp in H<sub>2</sub>O/EtOH (5%) for two hours showed a high photostability of these compounds distinctive for Si-rhodamines and comparable to the photostable cyanine dye Nile Blue (ESI-figure 31).<sup>34, 35</sup> The dye **9** shows a very high photostability (4% degradation) whereas SiR **10** has only a decrease of 15% in absorption after two hours irradiation.

We also determined the limit of detection for optical imaging using a conventional, small animal optical imaging scanner. Specifically, we recorded an IVIS-image with different amounts of rhenium complex **10** (figure 2b), indicating that 1 nmol of the probe can be detected without difficulty. This value compares well with the sensitivity of conventional optical fluorophores employed for *in vivo* applications.<sup>36</sup> The stability of complex **10** was assessed in aqueous solution. The rhenium(II) d<sup>6</sup>-low-spin complex shows robust stabilities in PBS/EtOH (5%) at room temperature and at 37 °C, with no decomplexation observed after 24 hours (ESI table 1). Similar results were observed in challenge experiments with 1 mM histidine in PBS/EtOH (5%) at 37 °C, where complex **10** did not show any decomposition after 24 hours either. The high stability of **10** motivated us to pursue the synthesis for the corresponding <sup>99m</sup>Tc-radiolabelled analogue.

Technetium-99m complexation experiments with ligand **9** were performed under the conditions shown in figure 3a.

[<sup>99m</sup>Tc(CO)<sub>3</sub>(H<sub>2</sub>O)<sub>3</sub>]<sup>+</sup> was synthesized in accordance with the procedure of Alberto et al.<sup>37, 38</sup>

The technetium-99m complexed Si-rhodamine **11** was synthesized by incubation of 87 nmol ligand **9** with 81.4 MBq (2.2 mCi) [<sup>99m</sup>Tc(CO)<sub>3</sub>(H<sub>2</sub>O)<sub>3</sub>]<sup>+</sup> for 1 hour at 75 °C in an aqueous solution. The desired complex was isolated with a radiochemical yield of 59%, a radiochemical purity greater than 98% and a molar activity of 551 MBq/μmol (3a). The determination of the partition coefficient of **11** with the shake flask assay showed a value for log D<sub>pH=7.4</sub> = 1.11, indicating that the complex **11** has increased lipophilic character.

The comparison of the retention times of Re-complex **10** (UV-detection at 254 nm,  $R_t$  = 12.5 min) and the technetium-99m-complex (decay counts with  $\gamma$ -detection,  $R_t$  = 12.6 min)

confirms the identity of the desired final complex **11** (figure 3b).

Complex **11** was isolated using analytical HPLC and was redissolved in PBS/EtOH (5%) to determine the stability in aqueous solution. No additional peaks were observed, indicating good compound stability even after six hours of incubation. A serum stability test at 37 °C by incubation of **11** in human serum plasma showed high stability even after 24 hours analysed by Radio-TLC (ESI table 3).

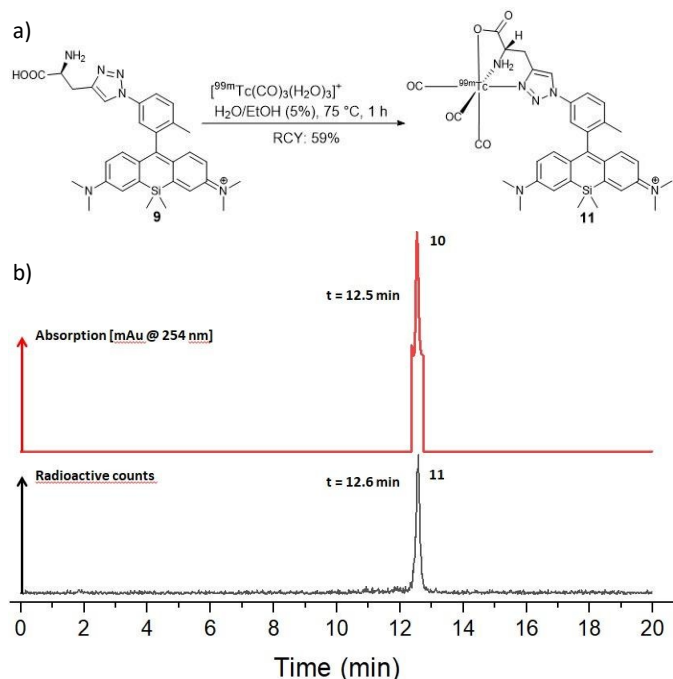


**Figure 3:** a) Radiolabelling reaction of ligand **9** with a highly reactive  $[^{99m}\text{Tc}(\text{CO})_3(\text{H}_2\text{O})_3]^+$ -complex in aqueous solution. b) Overview of the HPLC-trace of Re-complex **10** as a non-radioactive surrogate [UV, 254 nm] with a retention time of 12.5 min and the radio-HPLC-trace of the technetium-99m complex **11** [ $\gamma$ -detector, radioactive counts] with a retention time of 12.6 min. **11** was obtained in a radiochemical yield of 59% with a radiochemical purity of >98% after purification on an analytical HPLC with deionized water and acetonitrile containing 0.1% TFA each.

In conclusion, we here report on the first  $^{99m}\text{Tc}$ -radiolabelled small-molecule near-infrared Si-rhodamine fluorophore **11**. The novel, (radio)metal complexed fluorescent dyes **10** and **11** were successfully characterized. The technetium-99m and rhenium complexed Si-rhodamines can be easily synthesized and show excellent NIR optical properties, are stable under physiological conditions, in PBS, as well as in challenge experiments with histidine and additionally in human serum. Fluorophore **11** has the potential to be further combined with conventionally used, polydisperse  $^{99m}\text{Tc}$ -nanocolloids for sentinel lymph node (SNL) detection. In a next step the here presented and characterized non-targeted Si-rhodamines **10/11** will be further functionalized for their conjugation to different binding vector molecules to explore their potential of selective enrichment in (tumor) cells and tissues.

### Conflicts of interest

The authors have no conflicts to declare.

### Acknowledgements

View Article Online  
DOI: 10.1039/D0DT01084G

This work was supported by the Wilhelm Sander Stiftung for a grant on bimodal tumor tracers, grant 2018.024.1 (K. K. and C. S. K.) and the NIH, grant R00HL125728 (E. B.). Brett Vaughn is acknowledged for preparation of the technetium-99m-tricarbonyl precursor. Christian Jentschel is acknowledged for scientific support. T. K. acknowledges the FAZIT-Stiftung and the Helmholtz-International Graduate School for Cancer Research for financial support. Martin Schäfer, Dr. Aubry Miller and Dr. Sven Stadlbauer are gratefully thanked for helpful scientific discussions. Heidelberg University and Prof. Peter Comba are thanked for providing IR- and NMR-measurements.

### References

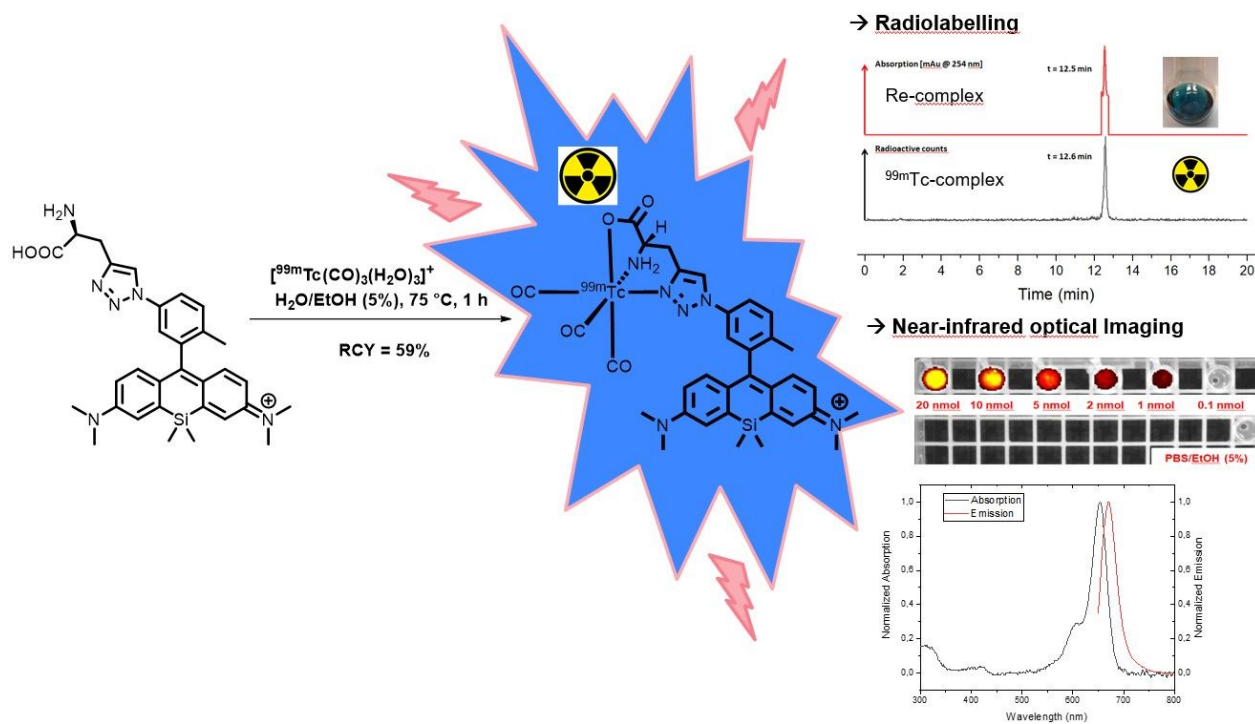
1. J. O. Escobedo, O. Rusin, S. Lim and R. M. Strongin, *Curr Opin Chem Biol*, 2010, **14**, 64–70.
2. V. N. Belov, C. A. Wurm, V. P. Boyarskiy, S. Jakobs and S. W. Hell, *Angew Chem Int Ed Engl*, 2010, **49**, 3520–3523.
3. S. Zhu, Q. Yang, A. L. Antaris, J. Yue, Z. Ma, H. Wang, W. Huang, H. Wan, J. Wang, S. Diao, B. Zhang, X. Li, Y. Zhong, K. Yu, G. Hong, J. Luo, Y. Liang and H. Dai, *Proc Natl Acad Sci U S A*, 2017, **114**, 962–967.
4. A. L. Antaris, H. Chen, S. Diao, Z. Ma, Z. Zhang, S. Zhu, J. Wang, A. X. Lozano, Q. Fan, L. Chew, M. Zhu, K. Cheng, X. Hong, H. Dai and Z. Cheng, *Nat Commun*, 2017, **8**, 1–11.
5. T. Ikeno, T. Nagano and K. Hanaoka, *Chem Asian J*, 2017, **12**, 1435–1446.
6. S. Luo, E. Zhang, Y. Su, T. Cheng and C. Shi, *Biomaterials*, 2011, **32**, 7127–7138.
7. D. Y. Zhang, S. Singhal and J. Y. K. Lee, *Neurosurgery*, 2019, **85**, 312–324.
8. R. Weissleder, *Nat Biotechnol*, 2001, **19**, 316–317.
9. N. Ando, H. Soutome and S. Yamaguchi, *Chem Sci*, 2019, **10**, 7816–7821.
10. A. Godard, G. Kalot, J. Pliquett, B. Busser, X. Le Guevel, K. D. Wegner, U. Resch-Genger, Y. Rousselin, J. L. Coll, F. Denat, E. Bodio, C. Goze and L. Sancey, *Bioconjug Chem*, 2020, **31**, 1088–1092.
11. E. Bodio, F. Denat and C. Goze, *J Porphy Phthalocya*, 2020, **23**, 1159–1183.
12. Y. Koide, Y. Urano, K. Hanaoka, W. Piao, M. Kusakabe, N. Saito, T. Terai, T. Okabe and T. Nagano, *J Am Chem Soc*, 2012, **134**, 5029–5031.
13. Y. Koide, Y. Urano, K. Hanaoka, T. Terai and T. Nagano, *ACS Chem Biol*, 2011, **6**, 600–608.
14. R. Weissleder and V. Ntziachristos, *Nat Med*, 2003, **9**, 123–128.
15. J. Culver, W. Akers and S. Achilefu, *J Nucl Med*, 2008, **49**, 169–172.
16. G. M. van Dam, G. Themelis, L. M. Crane, N. J. Harlaar, R. G. Pleijhuis, W. Kelder, A. Sarantopoulos, J. S. de Jong, H. J. Arts, A. G. van der Zee, J. Bart, P. S. Low and V. Ntziachristos, *Nat Med*, 2011, **17**, 1315–1319.
17. Z. Lu, T. T. Pham, V. Rajkumar, Z. Yu, R. B. Pedley, E. Arstad, J. Maher and R. Yan, *J Med Chem*, 2018, **61**, 1636–1645.
18. U. Seibold, B. Wangler, R. Schirmacher and C. Wangler, *Biomed Res Int*, 2014, **2014**, 153741.

19. Z. Li, T. P. Lin, S. Liu, C. W. Huang, T. W. Hudnall, F. P. Gabbai and P. S. Conti, *Chem Commun (Camb)*, 2011, **47**, 9324–9326.
20. S. Liu, D. Li, Z. Zhang, G. K. Surya Prakash, P. S. Conti and Z. Li, *Chem Commun (Camb)*, 2014, **50**, 7371–7373.
21. M. Schottelius, M. Wirtz, M. Eiber, T. Maurer and H. J. Wester, *EJNMMI Res*, 2015, **5**, 68.
22. S. Robu, M. Schottelius, M. Eiber, T. Maurer, J. Gschwend, M. Schwaiger and H. J. Wester, *J Nucl Med*, 2017, **58**, 235–242.
23. S. R. Banerjee, M. Pullambhatla, Y. Byun, S. Nimmagadda, C. A. Foss, G. Green, J. J. Fox, S. E. Lupold, R. C. Mease and M. G. Pomper, *Angew Chem Int Ed Engl*, 2011, **50**, 9167–9170.
24. T. L. Mindt, H. Struthers, L. Brans, T. Anguelov, C. Schweinsberg, V. Maes, D. Tourwe and R. Schibli, *J Am Chem Soc*, 2006, **128**, 15096–15097.
25. S. Liu and D. S. Edwards, *Chem Rev*, 1999, **99**, 2235–2268.
26. G. Lukinavicius, K. Umezawa, N. Olivier, A. Honigmann, G. Yang, T. Plass, V. Mueller, L. Reymond, I. R. Correa, Jr., Z. G. Luo, C. Schultz, E. A. Lemke, P. Heppenstall, C. Eggeling, S. Manley and K. Johnsson, *Nat Chem*, 2013, **5**, 132–139.
27. C. R. Bertozzi and P. Shieh, *US Patent US9410958B2*, 2015.
28. P. Shieh, M. S. Siegrist, A. J. Cullen and C. R. Bertozzi, *Proc Natl Acad Sci U S A*, 2014, **111**, 5456–5461.
29. H. Struthers, B. Spingler, T. L. Mindt and R. Schibli, *Chem Eur J*, 2008, **14**, 6173–6183.
30. J. G. Darab and P. A. Smith, *Chemistry of Materials*, 1996, **8**, 1004–1021.
31. L. H. Davies, B. B. Kasten, P. D. Benny, R. L. Arrowsmith, H. Ge, S. I. Pascu, S. W. Botchway, W. Clegg, R. W. Harrington and L. J. Higham, *Chem Commun (Camb)*, 2014, **50**, 15503–15505.
32. E. E. Langdon-Jones, N. O. Symonds, S. E. Yates, A. J. Hayes, D. Lloyd, R. Williams, S. J. Coles, P. N. Horton and S. J. Pope, *Inorg Chem*, 2014, **53**, 3788–3797.
33. W. L. Turnbull, L. Yu, E. Murrell, M. Milne, C. L. Charron and L. G. Luyt, *Org Biomol Chem*, 2019, **17**, 598–608.
34. Y. Koide, Y. Urano, K. Hanaoka, T. Terai and T. Nagano, *J Am Chem Soc*, 2011, **133**, 5680–5682.
35. V. Martinez and M. Henary, *Chemistry*, 2016, **22**, 13764–13782.
36. S. Hameed, H. Chen, M. Irfan, S. Z. Bajwa, W. S. Khan, S. M. Baig and Z. Dai, *Bioconjug Chem*, 2019, **30**, 13–28.
37. R. Alberto, K. Ortner, N. Wheatley, R. Schibli and A. P. Schubiger, *J Am Chem Soc*, 2001, **123**, 3135–3136.
38. C. C. Konkankit, B. A. Vaughn, S. N. MacMillan, E. Boros and J. J. Wilson, *Inorg Chem*, 2019, **58**, 3895–3909.

View Article Online  
DOI: 10.1039/D0DT01084G

**Table of contents entry:****Rhenium and technetium-complexed silicon rhodamines as near-infrared imaging probes for bimodal SPECT- and optical imaging**

Original:



The first technetium-99m tricarbonyl core labelled fluorescent Si-rhodamine and its rhenium analogue for bimodal SPECT- and near-infrared fluorescence imaging is presented.

4 cm x 8 cm:

